Influence of Breaking Waves on Scour Processes around Circular Offshore Wind Turbine Foundations

Frigaard, Peter; De Vos, Leen

Publication date:
2005

Document Version
Early version, also known as pre-print

Influence of breaking waves on scour processes around circular offshore wind turbine foundations.

by

Peter Frigaard and Leen De Vos
Aalborg University

INTRODUCTION

Scour and scour protection are major issues to consider when constructing offshore wind farms. The majority of wind farms to be built are situated in environments characterized by strong influence of tides, wind-induced currents and waves, both breaking and non-breaking. If the turbines are placed without protection on an erodible seabed, a scour hole will develop. The engineer can either include the scour in his design, or he can place a scour protection on the seabed. Which of the two solutions is the most attractive depends on the cost of providing scour protection compared with the extra cost of making the pile stronger/longer, extra cable dredging etc. The optimal solution will depend to a large extent on the maximal scour depth an unprotected foundation will experience during its lifetime.

For many years, engineers designing bridges have been used to taking into account scour around structures exposed to steady currents. The "Manual on scour at bridges and other hydraulic structures" by CIRIA (2002) is an example of a book giving a good overview of this topic. The typical fully-developed scour depth in a uniform current is 1 to 1.5 times the pile diameter, resulting in a typical maximum scour depth in the range of 5-8 m for a typical pile with a diameter equal to 5 m.
On the other hand, wave scour has not received the same amount of attention. Nevertheless, with the development of offshore wind farms, there has been a growing focus on wave scour. Two excellent books to give an overview of wave induced scour and scour caused by combined waves and currents are "Scour at marine structures" by Whitehouse (1998) and "The mechanics of scour in the marine environment" by Sumer and Fredsøe (2002).
It is generally known and accepted that scour around a pile caused by current only is decreased when non-breaking (short) waves are superimposed on the current. So far, little knowledge on the effect of breaking waves superimposed on a current is available. Bijker and De Bruyn (1988) measured greater scour depths (up to $S_e/D = 1.9$) when breaking waves are superimposed on a current, which is considerably (up to 46%) larger than the scour in the current-only situation. They relate the increase of the scour to the observed increase of the orbital velocity under breaking waves.

Today's practice has not yet been defined, but some engineers include possible wave breaking in their design by increasing scour depth for current alone. This simply means that the design scour depth is considered to be more than 1.5 times the pile diameter. This report includes an experimental study of scour processes in physical model as well as an experimental study using particle image velocimetry (PIV) technique and numerical modelling of bed velocities, looking at the influence of non-breaking, breaking and broken waves. It is demonstrated that scour depths are only little influenced by the breaking waves.

EXPERIMENTAL SET-UP

Scour tests

IS THERE AN APPENDIX DESCRIBING THE EXPERIMENTS? I GUESS YES? IS THERE STILL ROOM FOR A LITTLE PART ON IT HERE OR DO I JUST REFER TO ANOTHER APPENDIX/PART??

Tests in a length scale 1:30 were performed in a wave flume at the Hydraulics and Coastal Laboratory, Aalborg University. The flume is 18.7 m long and 1.2 m wide, see figure 1. A two-way pump able to circulate 650 l/s is mounted beneath the flume. It was possible to ensure a reasonably constant velocity profile.

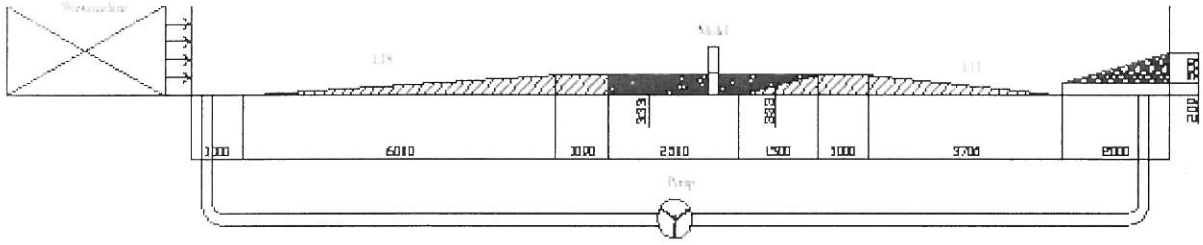

Figure 1. The wave flume. All measurements in millimetres.

The sloping bed is constructed in order to induce wave breaking. The bed slopes are made of concrete, the part in which the monopile model is built in consists of a 4 m long sand box filled with fine sand, d_{50} = 17 mm. Sand is also spread out in a thin layer across the slopes to simulate the natural bed sediment transport in the sandbox. A monopile model is fixed to the concrete bottom underneath the sand box. The diameter of the monopile varies between 0.10 m and 0.20 m.

In all tests a live bed condition is achieved. Scour holes are measured in a 1.5 cm by 1.5 cm grid using a laser profiler. The measured grid is 1.5 m long and 0.93 m wide. Waves and currents are measured beside the model. Waves are separated into incident and reflected waves. In Larsen et. al. (2005) a more detailed description of the test set-up can be found.

The present appendix focuses on the effects of breaking waves on scour. The test program described in table 1 includes both regular and irregular waves. The main purpose of the irregular tests is to study the effects of wave breaking by making comparisons with tests from literature, performed with non-breaking waves. The main purpose of the tests with regular waves is to make a comparison with the calculations in the numerical model.

Table 1. Test programme for the scour tests, irregular waves

Test no	Comments	Diameter of monopile D [m]	Significant wave height H_s [m]	Spectral peak period T_p [s]	Water depth seaward d_0 [m]	Water depth at pile h_t [-]	Current induced velocity U_c [m/s]
1.1	*breaking*	0.10	0.12	1.28	0.62	0.29	0.00
1.2	*waves, with*	0.10	0.12	2.01	0.62	0.29	0.00
1.3	*and without*	0.10	0.08	1.28	0.50	0.17	0.00
1.4	*unidirectional*	0.10	0.08	2.01	0.50	0.17	0.00
1.5	*current*	0.10	0.12	1.28	0.62	0.29	0.30
1.6		0.10	0.12	2.01	0.62	0.29	0.30

Test no	Comments	Diameter of monopile D [m]	Significant wave height H_s [m]	Spectral peak period T_p [s]	Water depth seaward d_0 [m]	Water depth at pile h_t [-]	Current induced velocity U_c [m/s]
3.1	*Regular*	0.20	0.10	1.28	0.50	0.17	0.00
3.2	*waves*	0.20	0.10	2.01	0.50	0.17	0.00
3.3		0.20	0.10	2.50	0.50	0.17	0.00

Particle image velocimetry

Particle image velocimetry is a quantitative imaging technique, which has known a rapid growth over the last two decades. It is particularly well suited for the study of wavy fluid flows which are characterized by unsteady free surfaces and internal motions, as is described by Grue et al. (2004). The main advantage of PIV is that an instantaneous 2 dimensional flow field can be quantified. This is done by adding seeding particles to the flow. The particles are lit twice in one plane by a laser in a short period (with time delay Δt). With a CCD camera these two moments are captured and the velocity field in the enlightened plane is extracted by a cross correlation analysis.

Tests were performed on a length scale of 1:100 in a wave flume of the department of civil engineering, Ghent University. The flume is 15 m long, 0.35 m wide and 0.60 m high and is made almost entirely out of glass walls, which allows taking images through the bottom plate. A piston type wave paddle is able to generate regular and irregular waves. A monopile model is built in at the end of the flume, just in front of an absorbing beach. The generated waves are measured by means of a capacitance type wave gauge just in front of the pile.

Both horizontal velocity profiles near the bottom (figure 2) as a vertical velocity profile through the centre of the pile (figure 3) were captured at different phases of a passing wave. Because of the limited space under the wave flume, a mirror is used to create the desired distance for the camera. A picture of the set-up is shown in figure 4.

The same test is repeated several times for two reasons. The first reason is to assess repeatability and an average of three tests is taken as a result; the second reason is to be able to take images at different phases of the passing wave.

A trigger was coupled to one of the wave gauges in front of the pile, in order to take a camera image at the exact same time over and over again. Due to a shift in the trigger delay, images are available with an interim of only 50 ms.

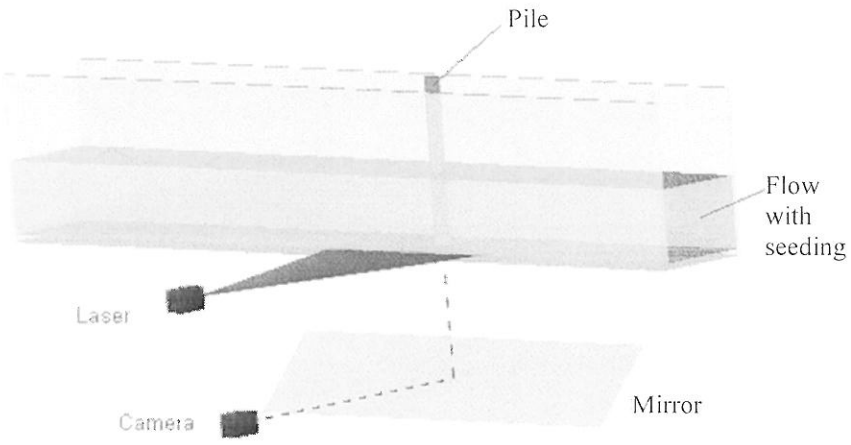

Figure 2. Principle of test set-up for velocities in a horizontal plane near the bottom.

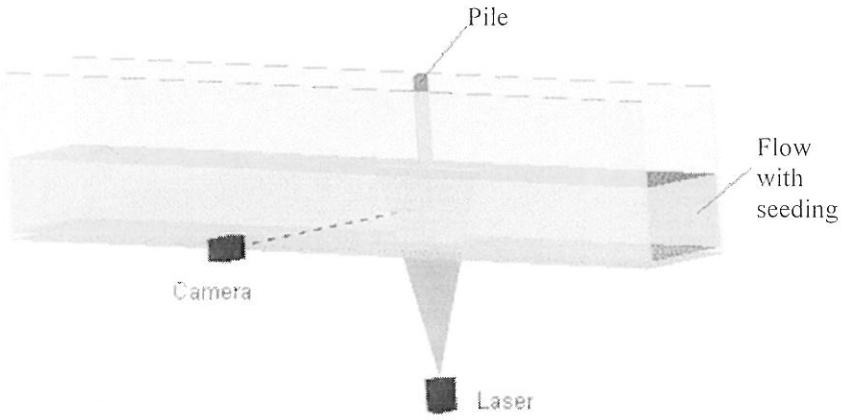

Figure 3. Principle of test set-up for velocities in a vertical plane through the centre of the pile.

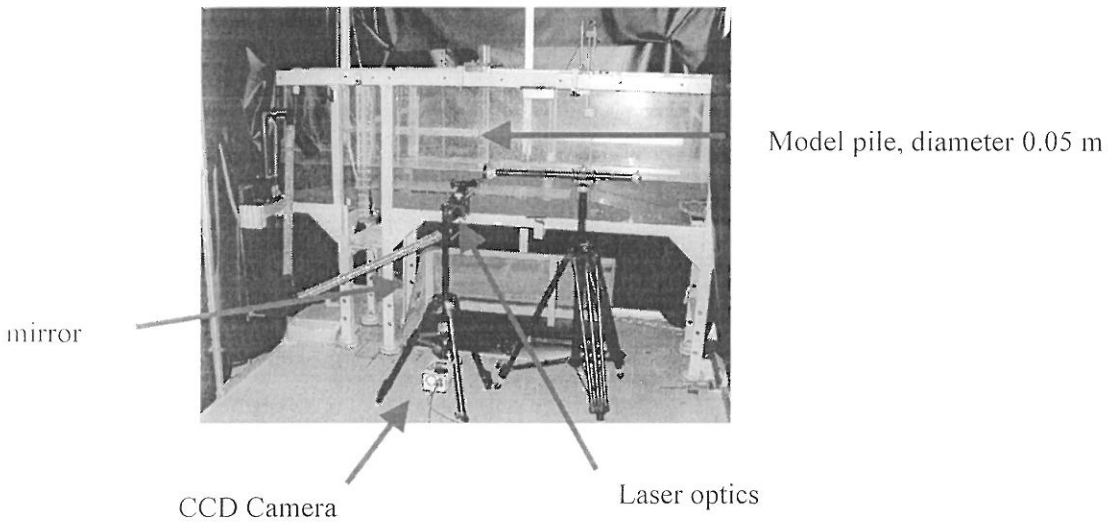

Figure 4. Picture of test set-up.

Two test series are performed, both of them with regular waves only (no current). The first tests are done with a non-breaking wave with a wave height of 0.1 m and a wave period of 1.52 s in a water depth of 0.20 m near the pile. In a second test series the velocity profiles due to a breaking wave were measured. In order to induce wave breaking, a platform was created and the pile characteristics were chosen in a way that the wave starts to break just in front of the pile: H = 0.1m, T = 1.48 s and d = 0.12 m near the pile.

The main purposes of the tests were to compare the amplification of the bed shear stress ($\tau \sim u^2$) for non-breaking and breaking waves and to compare the results with literature. After all, the sediment transport for non-cohesive sediment depends on the so called shields parameter, which expresses the ratio between the bed shear stress (driving forces) and the gravity (stabilizing forces): $\theta = \dfrac{\tau}{gd_{50}\rho(s-1)}$

Numerical modelling

The numerical investigations are based on the three-dimensional Navier-Stokes solver NS3. The method has been described in Mayer et al. (1998), Emarat et al. (2000), Nielsen and Mayer (2004), and Christensen et al. (2005).

The spatial discretization is based on the finite-volume approach on a multi-block grid. The time integration of the Navier-Stokes equations is performed by application of the fractional step method. Figure 5 shows an example of the multiblock grid used for the study. The grid consists of 12 blocks.

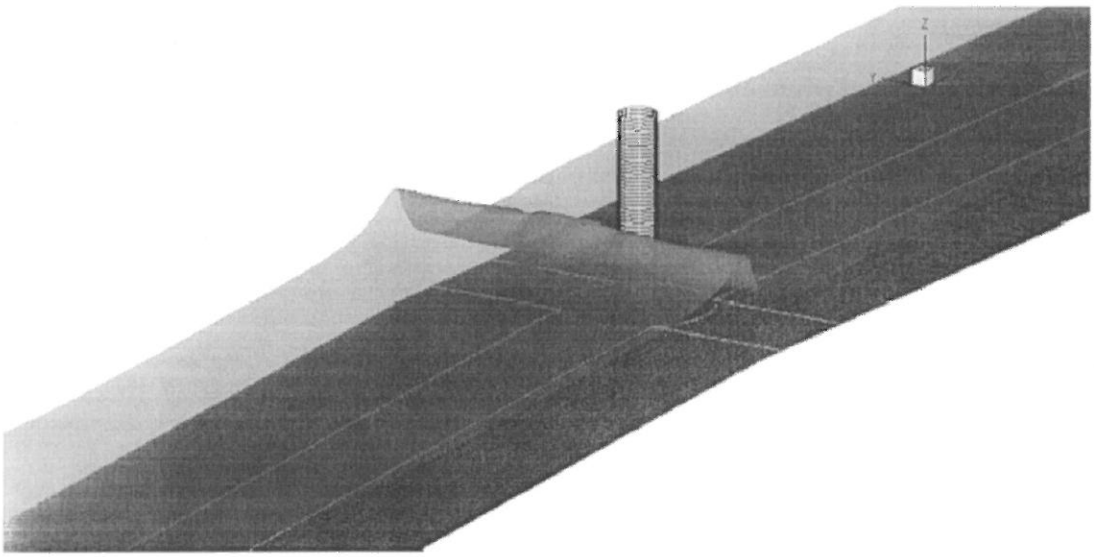

Figure 5. The multi-block structure of the computational domain shown at the bed (thick blue lines). The grid consists of twelve 3D blocks of structured data cells.

The free surface is resolved using a Volume-of-Fluid (VOF) description, with an improved scheme for the advection of the conservative quantity, F, cf. Ubbink (1997).
The scour development is mainly governed by the flow close to the seabed and the seabed properties. In order to study the influence from breaking waves, the flow is examined numerically for the same near-bed properties with and without the influence of breaking waves. The numerical model has been set up for the same near-bed flow properties as the physical scour experiments (regular waves).

The NS3 has been set up for 10 simulations (table 2) described by the parameters explained in figure 6.

D_cyl: Depth at the cylinder
D_in: Depth at inlet boundary
H_cyl: Shoaled wave height at the cylinder
H_in_bound: Wave height at inlet boundary
T: Wave period
L_cyl: Wave length at cylinder
Ks: Shoaling coefficient
Dia: Diameter of the cylinder
Dist: Distance from centre of the cylinder to the beginning of the slope

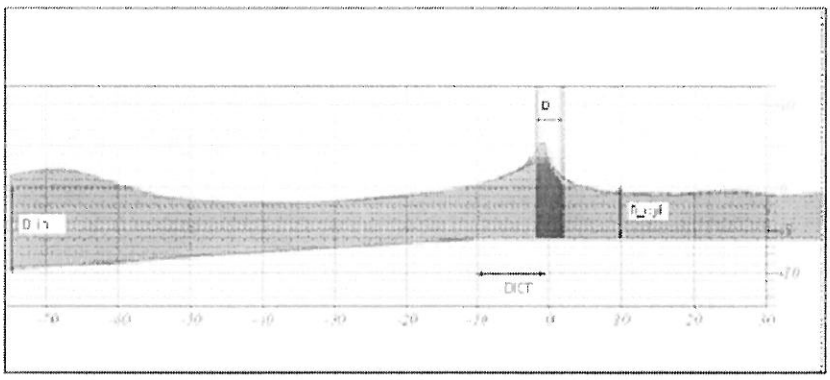

Figure 6. Definition of numerical parameters.

Table 2. Numerical test parameters.

Simu-lation	D_cyl	H_cyl	T	Dia	KC	H_cyl/ D_cyl	L_cyl	D_in	Ks	H_in_ bound	Slope	Dist
1	6	4	8	4	4.47	0.67	57.5	10	0.9392	3.757	1:20	10
2	6	4	8	2	8.93	0.67	57.5	10	0.9392	3.757	1:20	10
3	12	5.496	9	4	4.47	0.458	87.9	16	0.9794	5.383	1:20	10
4	12	5.496	9	2	8.93	0.458	87.9	16	0.9794	5.383	1:20	10
5	6	4	8	4	4.47	0.67	57.5	10	0.9392	3.757	1:20	15
6	6	4	8	2	8.93	0.67	57.5	10	0.9392	3.757	1:20	15
7	6	4	8	4	4.47	0.67	57.5	10	0.9392	3.757	1:20	25
8	6	4	8	2	8.93	0.67	57.5	10	0.9392	3.757	1:20	25
9	6	4	8	4	4.47	0.67	57.5	10	0.9392	3.757	1:20	50
10	6	4	8	2	8.93	0.67	57.5	10	0.9392	3.757	1:20	50

The KC number is found from the near-bed orbital velocities, determined by stream function theory, assuming regular waves, a constant water depth equal to the water depth at the pile (D_cyl), a wave height equal to the wave height at the pile (H_cyl) and a wave period T.
For the numerical modelling, the main purpose was to investigate the influence of the wave breaking on the bed shear stress and to compare results with the scour experiments.

EXPERIMENTAL RESULTS

Scour tests

The largest scour depths are developed during tests 1.5 and 1.6. In figure 7 the developed scour hole in test 1.5 can be seen (picture and profile measurement at the end of the test). Please note that in the picture, the upper part of the pile has been temporarily removed in order to make the profiling.

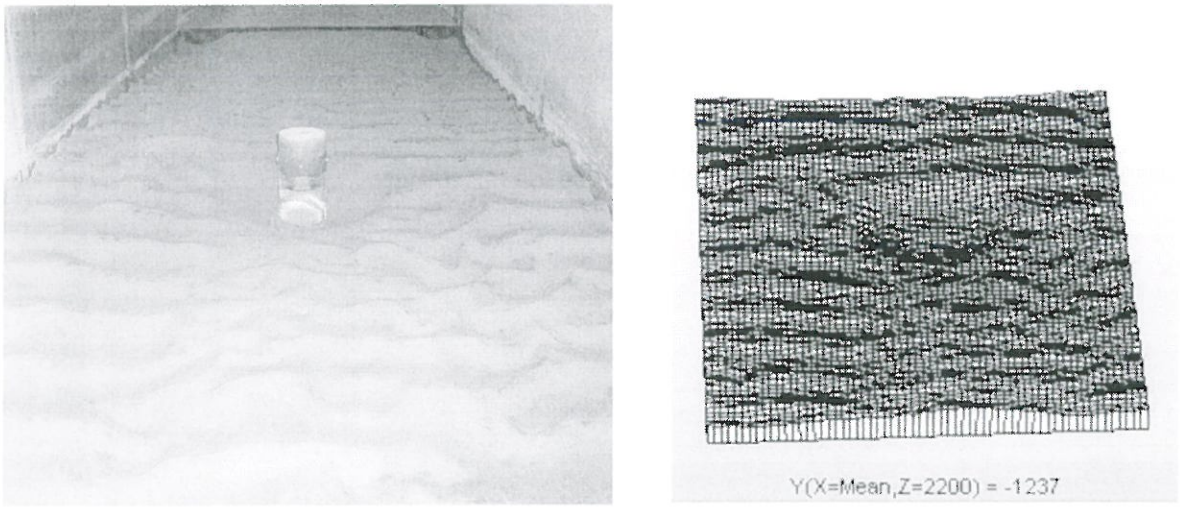

Figure 7. Picture and profiler measurement showing scour hole after 1500 waves. Test 1.5.

All results are summarized in table 3 (irregular waves) and table 4 (regular waves). The largest scour depth that is measured is S/D = 0.78.

Table 3. Results from physical tests, irregular waves.

Test no	Diameter of monopile D [m]	Significant wave height H_s [m]	Spectral peak period T_p [s]	Water depth at pile h_t [-]	Current induced velocity U_c [m/s]	Scour depth S [m]	Relative scour depth S/D [-]
1.1	0.10	0.11	1.31	0.29	0.00	0.012	0.120
1.2	0.10	0.12	1.97	0.29	0.00	0.020	0.200
1.3	0.10	0.07	1.28	0.17	0.00	0.011	0.110
1.4	0.10	0.08	1.97	0.17	0.00	0.014	0.140
1.5	0.10	0.11	1.31	0.29	0.30	0.078	0.780
1.6	0.10	0.12	1.97	0.29	0.30	0.078	0.780

Table 4. Results from physical tests, regular waves.

Test no	Diameter of monopile D [m]	Wave height H [m]	Period T [s]	Water depth at pile h_t [-]	Current induced velocity U_c [m/s]	Scour depth S [m]	Relative scour depth S/D [-]
3.1	0.20	0.10	1.28	0.17	0.00	0.019	0.095
3.2	0.20	0.11	2.01	0.17	0.00	0.032	0.160
3.3	0.20	0.09	2.50	0.17	0.00	0.026	0.260

Using the methodology given by Sumer and Fredsøe (2002), it is possible to compare the results with the results for the non-breaking waves listed by Sumer and Fredsøe (2002). In table 5, the Keulegan Carpenter number KC, U_{cw} and the Shields parameter θ are listed, with $U_{cw} = \frac{U_c}{U_c + U_m}$.

Table 5. Calculated KC, U_{cw} and θ values for the different test cases.

Test no	KC	U_{cw}	θ
1.1	3.1	0	0.058
1.2	6.0	0	0.108
1.3	3.1	0	0.103
1.4	5.6	0	0.164
1.5	3.1	0.61	0.186
1.6	6.0	0.51	0.241

Figure 8 shows the measured maximum scour depth S (S/D in dimensionless form) as a function of the combined wave-current velocity U_{cw}.

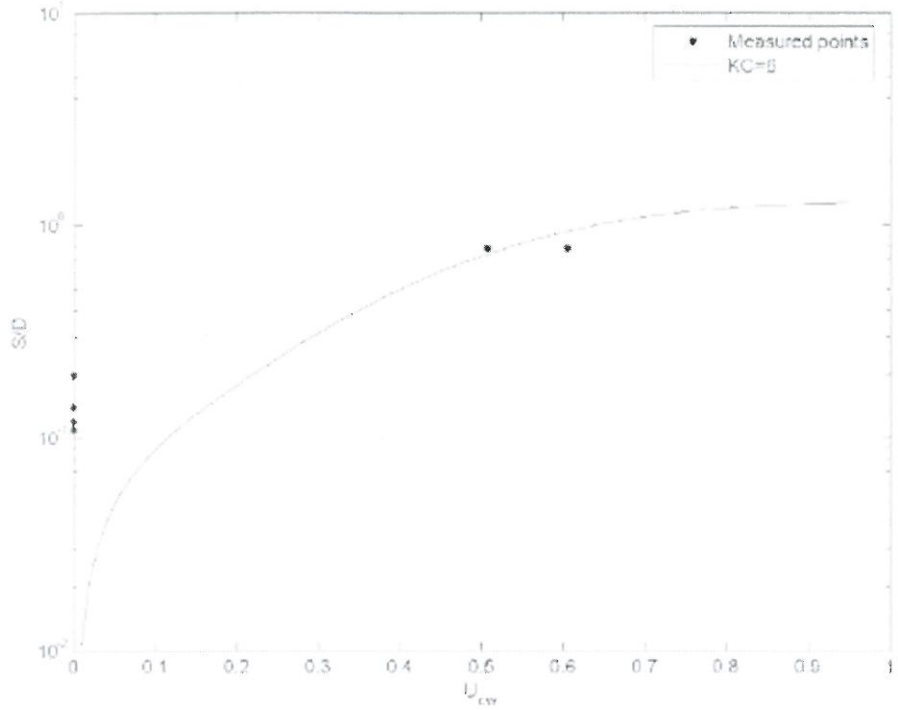

Figure 8. Comparison of predicted scour for non-breaking waves calculated according to Sumer and Fredsøe, with KC=6, and measured scour for breaking waves.

From figure 8, it can be deduced that the formed scour holes are comparable to those predicted by Sumer et al. (2002), which are valid for non-breaking waves. This would imply that there would be no to little influence of the wave breaking on the depth of the scour hole. It should be emphasized however that the tests are performed with irregular waves, which implies that the wave breaking does not occur for every wave, neither as it occurs at the same distance from the pile. This might influence the development of the scour hole in a less negative way than when each wave would brake at the exact same location. Irregular waves are however a much better simulation of a prototype situation.

Particle image velocimetry

In table 6, the test parameters and maximum measured velocities are reported. The KC numbers are respectively 9.4 for the non-breaking wave and 12.4 for the breaking wave. The amplification of the bed shear stress is calculated, assuming that $\tau = \frac{1}{2}\rho f_w U^2$ (or $\tau \sim U^2$), with a constant friction factor f_w.

Table 6. Results from PIV tests, regular waves.

Test no	Diameter of monopile D [m]	Significant wave height H [m]	Spectral peak period T_p [s]	Water depth at pile d [-]	Comment -	Keulegan Carpenter number KC [-]	Maximum orbital velocity away from pile U_m [m/s]	Maximum measured velocity near pile $U_{m,pile}$ [m/s]	Amplification of maximum bed shear stress α [–]
1	0.05	0.10	1.52	0.20	non breaking	9.4	0.31	0.6	3.8
2	0.05	0.10	1.48	0.12	breaking	12.4	0.42	0.85	4.1

From literature we know that for KC numbers > 7, vortex shedding will occur (Sumer et al., 1997). This vortex shedding can indeed clearly be seen on the velocity images which are taken in the horizontal plane (figure 9 and figure 10).

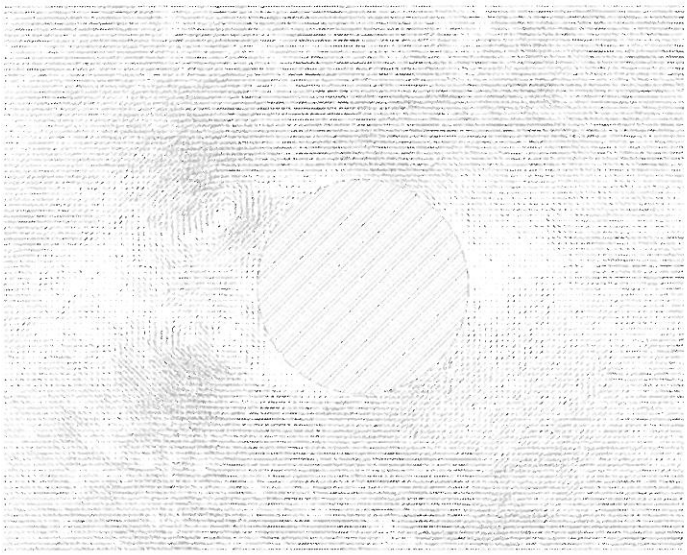

Figure 9. Velocity filed around the pile, near the bottom; non-breaking wave. Average velocity: 0.1 m/s, maximum velocity 0.3 m/s (close-up around the pile).

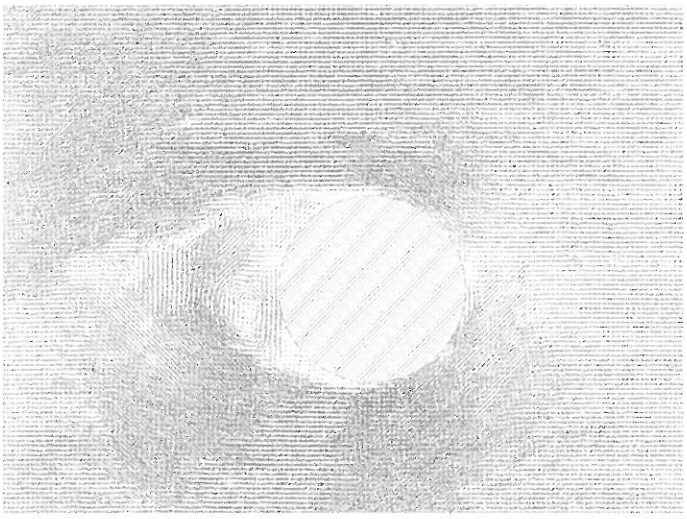

Figure 10. Velocity filed around the pile, near the bottom; breaking wave. Average velocity: 0.2 m/s, maximum velocity 0.4 m/s (close-up around the pile).

The amplification of the bed shear stress for two different KC numbers (non-breaking waves) is shown in figure 11. From this we can deduce that for both tests, the maximum amplification around the pile should lie around 4 (KC = 10.3 in figure 7). From table 6 we can see that for the test with the non-breaking wave, the amplification is 3.8 for the non-breaking wave and 4.1 for the breaking wave. This lies very close to the value of 4.

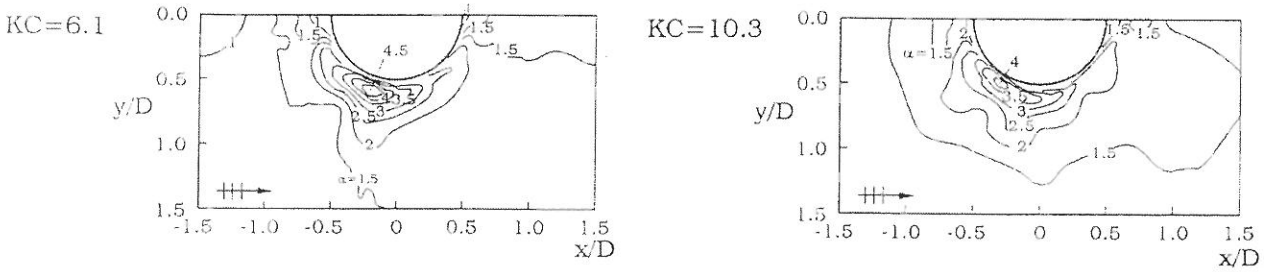

Figure 11. Amplification of bottom shear stresses around a cylindrical pile (Sumer et al, 2002)

In figure 12 and 13, the moment of maximum velocity is shown both for the non-breaking and the breaking wave. Both the vertical picture and the processed vertical and horizontal images are shown.

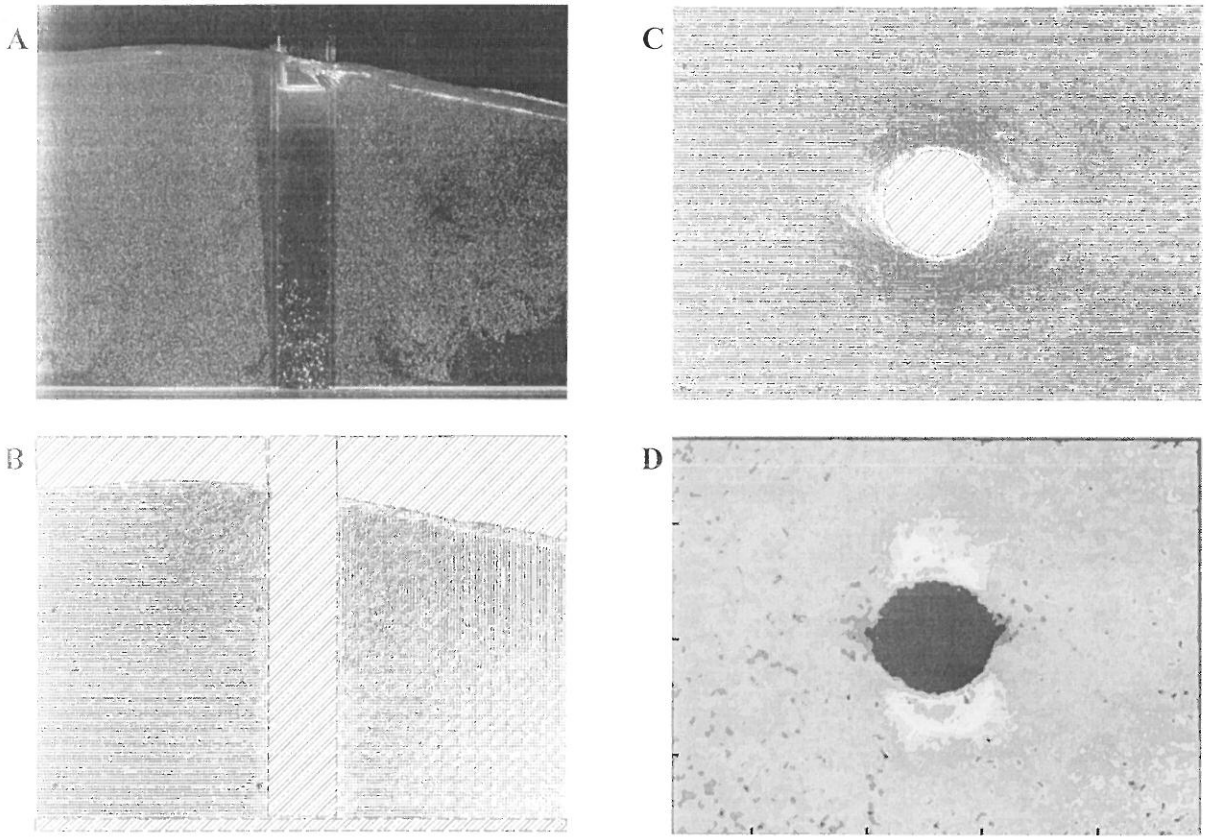

Figure 12. Snapshot of moment with maximum velocities; non-breaking wave
A: vertical picture
B: velocity vectors in vertical field
C: velocity vectors in horizontal field
D: Contour plot of velocities in horizontal field

From figure 12, it can be seen that for the non-breaking wave, the maximum bottom velocity is reached at the moment that the wave top reaches the pile. For the breaking wave (figure 13) the maximum bottom velocity occurs when the breaking crest has just passed the pile.

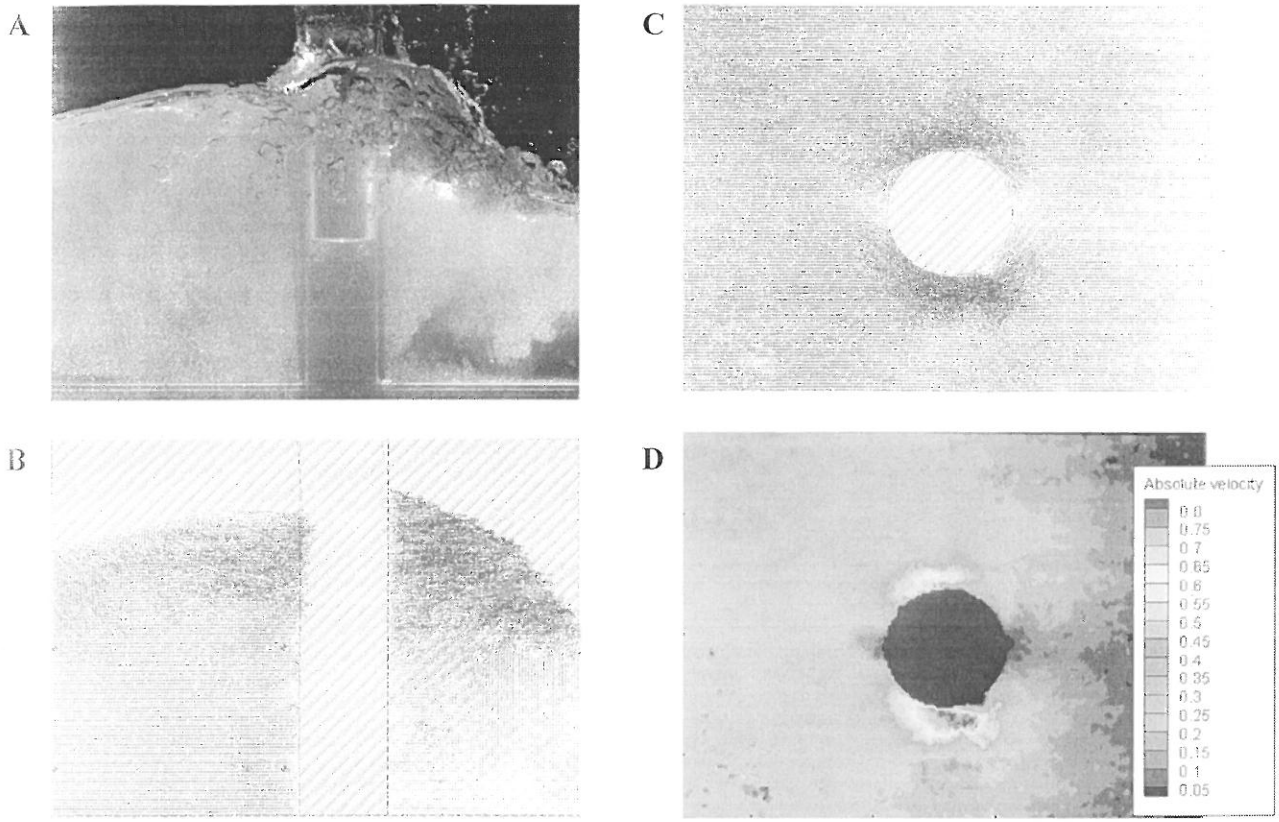

Figure 13. Snapshot of moment with maximum velocities; breaking wave
A: vertical picture
B: velocity vectors in vertical field
C: velocity vectors in horizontal field
D: Contour plot of velocities in horizontal field

Both the velocity profiles and the amplification of the bottom shear stress near the pile are comparable for non-breaking and the breaking wave. In figure 13.B it can be seen that, although velocities are very high (much higher than for the non-breaking wave) in the top part of the breaking crest (up to 1.7 m/s), the large increase in velocity is always limited to approximately two thirds of the water depth. This means that the influence of the increased turbulence and velocity due to the breaking of the wave does not reach the bottom.

Numerical results

Figure 14 shows a snapshot of a wave hitting the pile, for simulation 1 and 2. In figure 15 a snapshot of the near-bed velocities for simulation 1 and 2 are shown. The simulations show that separation does not form for the large diameter pile (KC = 4.5), while it does develop for the small diameter (KC = 9); this is in accordance with flume observations, see for example Sumer and Fredsøe (2002) and as explained above.

In order to study the influence of wave breaking, the bed friction velocities have been compared for simulation 2, where the wave is just about to break, but has not broken yet, and simulation 8, where the breaking process is at a mature stage. A quadratic relation between the bed shear stresses and the near-bed velocities: $\tau = 0.5\rho f_w U_{bed}^2$ has been assumed. The

friction velocity can be determined from this near-bed velocity U_{bed}: $U_f = \sqrt{0.5 f_w} U_{bed}$. Figure 16 shows the friction velocities, assuming a constant friction factor f equal to 0.01.

By comparing the friction velocities in the two cases, it is evident that wave breaking only has a small influence on bed shear stresses; there is even a tendency that the bed shear stresses are lower in case of wave breaking. This supports the experimental findings from the PIV measurements and the scour tests, finding that scour is only weakly dependent on wave breaking.

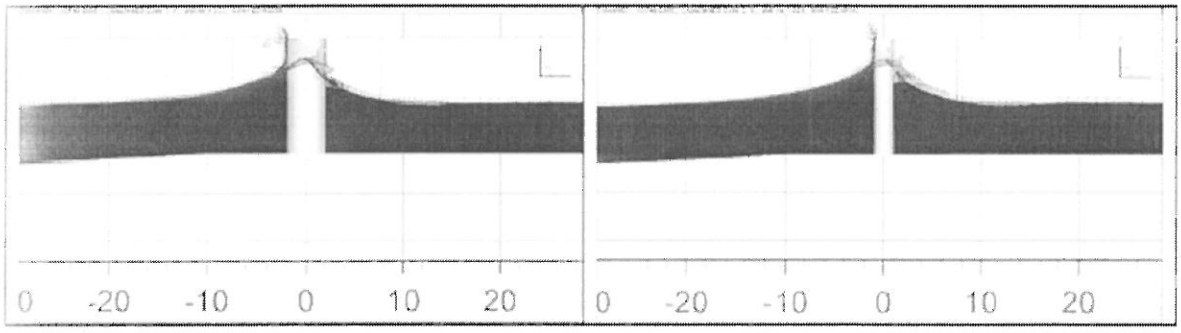

Figure 14. The wave hitting the cylinder at the same phase for simulation 1 (large pile diameter, left) and simulation 2 (small pile diameter, right).

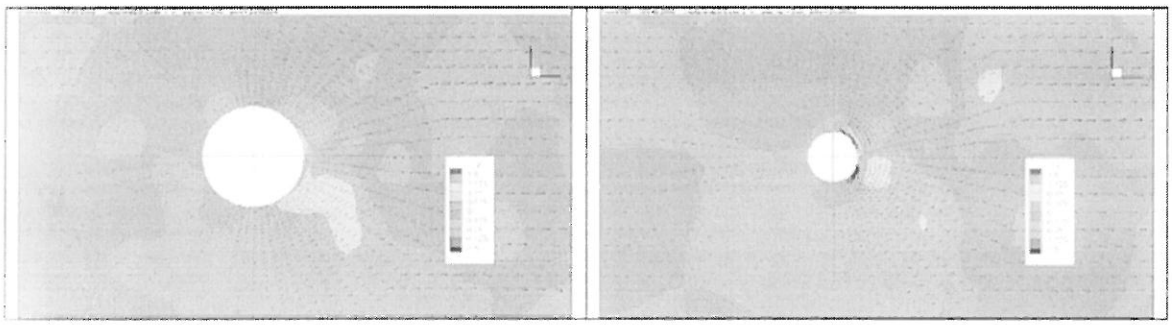

Figure 15. Snapshot of the bed velocities (m/s) for simulation 1 and 2, the colours indicate the flow velocity in the y direction (perpendicular to the wave propagation direction).

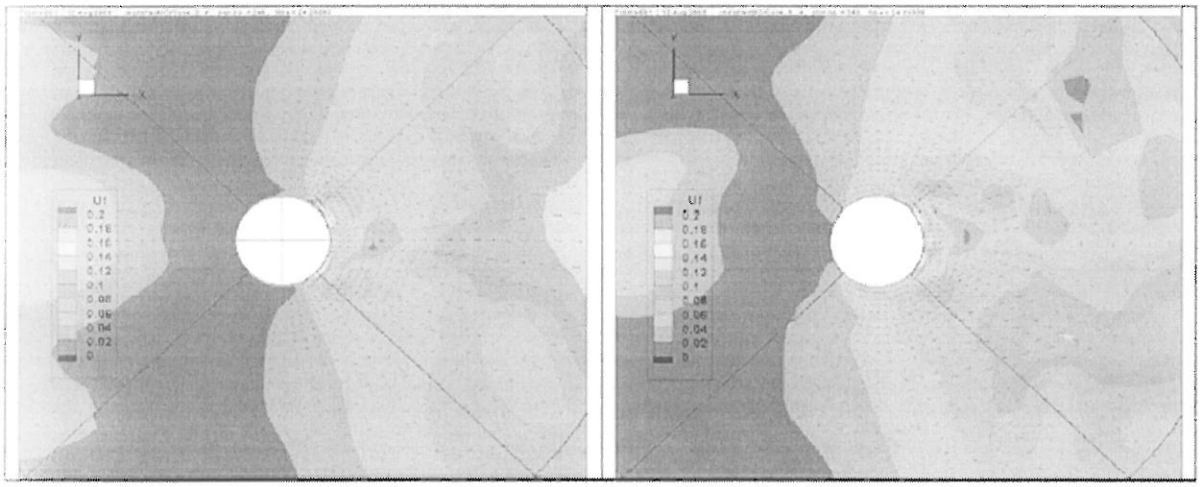

Figure 16. The friction velocity at the same phase for simulation 2 (left) and simulation 8 (right).

CONCLUSION

Normally the presence of waves will not increase but rather decrease the scour depths compared with situations where only currents are present.
In literature many equations for estimation of scour depths can be found. As a part of this project "Offshore vindmøller I stærk strøm" Jensen (2004) lists a comprehensive overview of existing formulas. Sumer (2002) reanalyzed a lot of data from literature, and came up with the very simple equation for the maximum scour depth S, S = 1.3 D. Most data related to non-breaking situations.
However, knowledge on the influence of breaking waves on scour depths is limited. Bijker and Bruyn (1988) wrote: *The depth of this scour is in the order of 1.5 times the pile diameter. In case of breaking waves this value can be, however, considerably higher. This paper gives a large influence on the scour prediction in breaking waves.*
In the present study, no such dependency was seen. Both the physical experiments as well as the numerical study show that the effect of breaking waves only has a small influence on the scour development: both bed shear stresses and scour depths in breaking waves and in non-breaking waves were comparable. Looking closer at the figures in the Bijker and Bruyn paper, it seems that it is not the presence of the pile that causes the larger scour depths, but it is the bed itself which is subjected to large changes due to the ripple formation and dynamics. A comparable experimental study of Carreiras et al. is described in Sumer et al. (2002). Here the effect of breaking waves on scour was studied experimentally with the aid of 5 experiments in which the pile was placed at a different position related to the point of wave breaking on a 1:20 sloping beach. The study shows that, depending on the position of the pile relative to the breaking point, the ripple formation and dynamics and the formation of a bar were found to have a main influence on the evolution of scour. The final bed changes resulted from the superposition of the large scale bed evolution due to wave breaking and the small scale bed scour.

Good agreement between physical tests and numerical calculations was shown. The numerical model seems to be able to pick up the correct physics.

REFERENCES

BIJKER E.W. AND DE BRUYN C.A. "Erosion around a pile due to current and breaking waves." Coastal Engineering, ASCE, 1988

CHRISTENSEN E.D., BREDDMOSE H. AND HANSEN E.A. "Extreme wave forces and wave run-up on offshore wind-turbine foundations." Presented at Copenhagen Offshore Wind 2005

EMARAT N., CHRISTENSEN E.D., FOREHAND D.I.M. AND MAYER S. "A study of plunging breaker mechanics by PIV measurements and a Navier-Stokes solver." Proc. Of the 27th Int. Conf. on Coastal Eng., ASCE, Sydney, Australian Vol. 1, pp 891-901, 2000

GRUE J., LIU P.L.-F. AND PEDERSEN G.K. "PIV and water waves", World Scientific, 2004

JENSEN M.S. "Offshore vindmøller I stærk strøm" Rambøll internal report. Reference no. 070001, 2004

LARSEN B.J., FRIGAARD P. AND JENSEN M.S. "Offshore Windturbines in Areas with Strong Currents." Hydraulics and Coastal Eng. No. 19. Aalborg University. ISBN 1603-9874, 2005

MAY R.W.P., ACKERS J.C., KIRBY A.M. "Manual on scour at bridges and other hydraulic structures" CIRIA, 2002

MAYER S., GARAPON A. AND SØRENSEN L.S. "A fractional step method for unsteady free-surface flow with application to non-linear wave dynamics." Int. Journal for Numerical Methods in Fluids, Vol. 28, No. 2, pp. 293-315, 1998

NIELSEN K.B., AND MAYER S. "Numerical prediction of green water incidents" Ocean Engineering, Vol 31, pp 363-399, 2004

SUMER B.M. AND FREDSØE, J. "The mechanics of scour in the marine environment." World Scientific, ISBN 981-02-4930-6, 2002

WHITEHOUSE, R. "Scour at marine structures." Thomas Telford Ltd, ISBN 0-7277-2655-2, 1998

NOTATION

d = water depth;
D = pile diameter;
d_{50} = median grain diameter;
f_w = friction factor;
g = gravitational acceleration;
H = wave height;
H_s = significant wave height;
KC = Keulegan Carpenter number, $KC = \frac{U_m T}{D}$;
s = ratio of densities of grain and water;
S = scour depth;
S_e = equilibrium scour depth;
T = wave period;
T_p = wave peak period;
U = velocity;
U_c = current velocity;
U_{cw} = velocity ratio, $U_{cw} = \frac{U_c}{U_c + U_m}$;
U_f = friction velocity;
U_m = amplitude of horizontal orbital velocity;
θ = Shields parameter, $\theta = \frac{\tau}{g d_{50} \rho (s-1)}$;
ρ = density of water;
τ = bed shear stress, $\tau = \frac{1}{2} \rho f_w U_m^2$.